Journal of Multidisciplinary Engineering Science and Technology (JMEST)
ISSN: 2458-9403
Vol. 8 Issue 7, July - 2021

Research and Analysis For The Resurgence Of The Solid & Composite Desiccant By Utilizing Solar Concentrator Of Scheffler

Bhanu Pratap Singh[1], Rahul Patel[2]

1. Research Scholar, Department Of Mechanical Engineering, Suyash Institute Of Information Technology, Gorakhpur, (U.P.), India, Affiliated To Dr. APJ Abdul Kalam Technical University, Lucknow, (U.P.), India

2. Assistant Professor, Department Of Mechanical Engineering, KIPM College Of Engineering & Technology, GIDA, Gorakhpur, (U.P.), India, Affiliated To Dr. APJ Abdul Kalam Technical University, Lucknow, (U.P.), India

***Abstract*—High humidity is significant solicitude in the equatorial area of the earth. The result is continuously increasing the haul of air in the dehumidification. The crucial worry of dehumidification system, layout is the energy utilization. Mostly the energy exhausted for the dehumidification is needed for the removal of availability from the air steam. The framework of desiccant, the dehumidification has received more concern in the last years because the substitute of the common dehumidification unit. The amount of humid air can be dehumidified excluding the accumulation through utilizing the desiccant dehumidification because there is a immediate relation between moist air and the desiccant dry.**

Resurgence of many saturated desiccant (based on wet) like the silica gel, operated alumina, operated charcoal and novel combination desiccant utilizing the solar concentrator of scheffler (SSC) has been suggested. Novelty performance gets more contrived by utilizing the solar radiation. Desiccant's surface temperature, the wind speed, and inceptive moisture availability for the Novelty of each desiccants SSC having an aperture area of 1.53m^2 that is designed & fabricated throughout the examination it has been established that a silica gel has greatest moisture availability (On the basis of dry) i.e. 0.2945 kg of water/Kg of dry desiccant followed by molecular strain, novel combined, operated alumina and operated charcoal having moisture availability of 0.2235, 0.18, 0.0672, and 0.057 kg of water / kg of dry desiccant respectively, the greatest rate of resurgence is 0.074 kg/hr performed in novel combine and high weight drop of about 22.70 % is gained in a silica gel. The time taken to regenerate operated alumina, silica gel, molecular strain, operated charcoal & novel desiccant composite are 90,160,140,120, & 110 minutes respectively.

Classical modeling for moisture ratio of novel composite desiccant by utilizing solar concentrator of the scheffler has also been expected. The drying curve achieved from practical data which is fitted to 12 of drying models for explanation of the behavior of novel desiccant composite. A best model is described by the "Midilli and kucuk" in related with the coefficient of the correlation (R) of 0.9940, & the root average square of error analysis (RSME) of 0.03120.

1. Introduction

Be in control of the humidity is an important of removing the availability from air for the use in manufacturing of or another non-standard methods as well conditioning the air. The content of moisture available in the air has an impact of building materials, comfort of the building inhabitants, as well as the work carried out in a facility, so as to control through, it is required. An air dehumidification is crucial view point for increasing durability of the objects because the dry air improves the methods, conditions of components in corresponding industries as well as in daily life for the example of sustenance generation, chemicals production of industry and pharmaceutical generation etc. An air dehumidification process is also utilized for Merchandise keep of the organic plant, the hygroscopic storage of basic materials, and also for packaging of the tool room. High humidity is native concern of equatorial area of the earth. It induces significantly enhancing in the charge of the air dehumidification. The crucial worry by the dehumidification substructure specification for energy use, mostly energy discharge for the dehumidification is needed for a rejection of availability from air because of the gathering availability remove the air is an adaptation state of the vapor. These are several ways of dehumidification utilization. The approach continuously for this is reliant on specific temperature as well as humidity conditions needed for the space and atmospheric conditions at this place. System utilized at the path of specific application has collected in light of their sufficiency and proficiency in achieving the Crave state. Simple for dehumidification integrate the use of compression cooling and the desiccants [1]. The dehumidification system of desiccant has achieved great consideration in preceding year as the substitute of common dehumidification structure. The humid air could be dehumidified in absence of water building build up by utilizing desiccant dehumidification; there is recent relation between the dry desiccant & moist air. The retrieve of desiccant can be feasible by utilizing the poor property retrieve heat source. Frequent Specialist has ventured to lower the retrieve temperature for executing the more efficiency chilling origin and by utilizing high efficiency of renewable the heating Origins. Sun heating is as example [2].

In dehumidification of desiccant set-up the wet air flow is allowed to follow by the material of desiccant, and subsequently dry air pull out from the material of desiccant. Continuing this method while ability of the

material of desiccant is to absorb moisture availability decreases and to maintain the framework persistently, the absorbed H_2O vapor should be removed. Though it is completed through heating material of desiccant to its temperature of resurgence, which is depending on type of the used material of desiccant. It is feasible replicate material of desiccant by a bad quality of heat origin like as natural gas and waste heat.

Creativity behind the work is for offer a safe option of little cost and long lasting solar based renewal material of desiccant for utilize in air dehumidification of crop drying uses when retaining up greater state of result and the properties.

It will enable solar powered of resurgence of the desiccant dehumidifiers solid to become a viable minimum cost option of food transportation utilizes in the tropical and subtropical areas. The desiccant is regenerated from utilizing the physical heat provided by the solar concentrator of scheffler. Novel desiccant may have a significant impact on decreasing the time required. Crop deprivation due to mycotoxin contamination from the improved drying, these techniques are currently being used in the regions of tropical and subtropical.

1.2 Dissertation outline

The following chapters award the work done in this dissertation. The first chapter introduces the importance of humidity control as well as the desiccant dehumidification setup. At the conclusion of the chapter outline additional a dissertation has been provided.

The second chapter provided a specific review of literature on the composite desiccant resurgence and solar concentrator of scheffler. Finally the chapter discusses the research gaps identified in the literature review, as well as the dissertation works objectives.

Chapter 3 goes over the complete mathematical calculations and design of a solar concentrator of scheffler which includes the design of frame of collector, crossbars and the depth of the ellipses of crossbars. This chapter also includes the construction of solar concentrator of scheffler as well as the cost estimation.

The fourth chapter compares the experimental performance of many solid and composite desiccants for the resurgence by using the solar concentrator of scheffler. The experimental setup installed at my residence Gorakhpur Uttar Pradesh ($26^0.78^I$ north's and $83^0.35^I$ East) is explain in detail as are the results. The measurement devices and the measuring instruments, as well as the experimental uncertainty have been described in this section. For all five cases, the experiment was carried out in March. This chapter also summarises the results and discussion for the different desiccants.

The mathematical analysis of drying curve of a composite desiccant is covered in chapter 5.12 drying models were fitted against the experimental data utilizing MATLAB as a statistical research tool in a pattern to determine the selected descriptive drying model for the desiccant composite. In chapter 6 of thesis, the conclusion and the recommendation are presented.

1.3 Conclusions

This chapter provides an overview of the need for humidity control and how the availability of moisture in air affects the building material, working environment and industries also. In last of this chapter an outline of the entire dissertation is also available.

2. Literature review

2.1 Introduction

The study described in the literature on resurgence of the desiccant material utilizing solar energy, the construction of composite desiccant to lower resurgence temperature and enhances the desiccant's moisture adsorption capacity. The solar concentrator of scheffler is a new member of the concentrating collector family presented.

The word mentioned in the literature is classified into three types

- Desiccant material resurgence
- Desiccant composite
- Solar concentrator of scheffler.

2.2 Resurgence of material of desiccant

Dupont et al. (1994) evaluated the enhancement of the silica gel, operated alumina and discovered as the silica gel could interchange 8.5 % more water on daily basis than the operated alumina. Next, it was shown the resurgence temperature of little more compared to above 78°C was enough to get such results [3].

The investigation of Singh and Singh in 1998, examined that the impact of recovery air temperature, bed-air velocity and number of racks on silica gel recovery in the multi shelf dehumidifier.

The range of recuperation air temperature was discovered to be 40-73°C. The air velocity in the bed varied. The velocity ranged from the 0.170m/s to 0.50m/s while the serial of racks ranges from 2.0 to 4.0.

Recuperation temperature of air and speed of bed-air for minimum energy details were 50°C and 0.170m/s respectively (number of racks is independent), with the healing time was shortened. Increase in rest period for each assessment of the serial of racks, the reduction in recuperation period was still inestimable [4].

In 1999 Tachajunta et al. investigated that resurgence of the silica gel through composite desiccant/gatherer utilizing electric operated light bulb to mimic an artificial solar radiation as the findings by help of the different integrated insulation levels & the discharge rate demonstrated as this was achievable. Sun heated air to renew silica gel in the humid tropical areas [5].

In 2001 chindaruksa et al. Built silica beds to extract an accurate estimate of the humidity of incoming air based on humidity material and the bed immersion. The bed covered inactively as a result of the silica induced air Channel. The bed recovered inactively as a result of induced air flow through the bed of silica gel, acting a chimney of solar. During the summer, the test for the both extreme adsorption as well as best recovery was carried out under real world settings. For the dynamic adsorption procedure the silica gel bed with a thickness of the 0.03 m & the wind stream of 0.02 kg/s is recommended. The silica gel recuperation utilizing a chimney of solar was about 0.041-0.062 kg/hr [6].

In 2007, Pramuang and Excell investigated the silica gel resurgence for use in an AC structure which has heated through a compound parabolic solar concentrator for Air heating with receiver and opening area of 0.45 and 1.40 m^2 respectively. The process of resurgence began at a temperature about 42°C. The collector of CPC gives temperature of up to 78°C and it may be utilized to recuperation of silica gel in two hours of a midday sun [7].

In 2015, Kumar et al. studied the resurgence of several desiccant materials as the operated alumina, the silica gel, and the operated charcoal in conjunction with a collector of parabolic shape. They came to the conclusion that the recuperation rate for silica was low when it is compared to operated Charcoal and operated alumina, gel was superior [8].

In 2012 Bajpai and Yadav investigated the resurgence rate of several solid desiccants. Operated charcoal, silica gel and operated alumina are examples of materials that can be used with evacuated tube of solar panels. The collector of an air in this study, air needed for retrieval heat is removed. Solar air collector tube with a surface area of 4.45m^2 is used. The desiccant was recovered at temperature ranging from 54.5°C to 68°C. Silica gel out performed operated alumina and operated carbon charcoal at more and the less flow esteems of retrieval and adsorption [9].

2.3 Desiccant composite

In 2000 Thoruwa and others Sought to develop sun powered recuperative clay $CaCl_2$ basis strong desiccant materials with minimum three efforts. The moisture adsorption and resurgence properties led to the conclusion that their employment in the sun based harvest drying was appropriate. Because of low regain temperature 100°C, air dehumidification is quite beneficial. These experiments have shown that the produced desiccants may be a viable alternative to utilize in crops drying and applications of air dehumidification in tropical countries [10].

In 1996, horuwa and others created a solar dryer based on desiccant for corn drying. The chamber was combined with the flat plate collector, and the corn was put over the material of desiccant. The desiccant utilized was made on site from $CaCl_2$ and clay of bentonite, of costly conventional desiccants. Adsorption capacity of the desiccant is 44%. It is suitable for recuperation at 46°C. Field testing and research facilities were utilized for determining of drying potential and give results that the prototype dryer has capacity of drying 80kg of fresh corn was reduced from 40 % to 16% in 24 hours [11].

Zhang and others (2005) initiated the group of silica gel - $CaCl_2$ composite adsorbents for the desiccant rotational wheel in the dehumidification structure. This practical study demonstrates that vapour adsorption qualities of the composite using $CaCl_2$ as infuge salt can be modified by the varying portion of salt interior the pores. The resurgence can be executed at moderately minimum temperature in the locality of 71°C and 118°C that enhances radically using the hot origin with a minimum temperature level, as to geothermal the waste heat and vitality based on sunlight [12].

Zhang and others in 2006 registered the silica gel (SG) desiccant balance and composite desiccant (SG-$CaCl_2$) for rotary wheel desiccant balance in order to balance their capacities to remove availability from wet air. Test details explain that the SG-$CaCl_2$ material can achieve the polyphony inside a short time and its hygroscopic level is greatly higher than the silica gel. It shows a great increment in humidity removal contrasted and the wheel of silica gel [13].

Tretiak and Abdallah improved and tested a desiccant consisting of the clay and $CaCl_2$ using several sorption, desorption cycles. Between sorption entry temperature ranges from 24°C to 38°C with contrast relative humidity in the range of 40%- 68% and air velocity from 0.18 to 0.80 m/s were tested usually. During desorption the channel air temperature ranges from 51°C to 58°C and air

velocity of around 0.31m/s and 0.68m/s were examined. Reverting state was resolved to mass of water sorbed through the clay of $CaCl_2$ desiccant and with a coefficient of the correlation of 0.91. Desiccant was established to perform well in the change test cycles [14].

Chan and others in 2012, synthesized solid desiccant zeolite and the $CaCl_2$ were investigated utilization in sunlight basis adsorption cooling structures a 0.45 g/g contrast in balance water follow in the locality of 20°C and 70°C at 880 Pascal was set down for the composite adsorbent. This was 400% of the zeolite under same conditions.

Mathematical simulation forecasts that an adsorption framework of cooling utilizing the solid composite adsorbent can be issued by a minimum grade thermal energy origin using the temperature range of 70°C -100°C [15].

Kumar and Yadav in 2015, practically investigated that a novel composite substance for the storage and creation of water from the climate air. The composite material has been blended by precipitation of $CaCl_2$ in the pores of the saw wood. It is established that water creation rate depends on the convergence of calcium chloride in saw wood.

More amount of water creation through the composite material having 61% concentration of 170 ml/kg/day [16].

Kumar and Yadav in 2016 practically investigated the heating performance of the solar based composite desiccant system of cooling. It consists of clear tube of sun powered water thermal solid composite desiccant bed of heat exchanger (CDBHE), the evaporative cooling unit and cooling tower composite desiccant is setup through jute and $CaCl_2$.

The high hot water's temperature adapted by a structure is 64.8°C which is enough to recover the material of composite desiccant. It has been established that the normal dehumidification enhances by 54.2% when using the cooling water. The coefficient of performance of desiccant cooling structure has been estimated to be 0.48 with the cooling level of 353.9w [17].

2.4 Solar concentrator of scheffler

In 2006 Scheffler found that around 51% of Sun energy can be used for cooking and established some ideas for the complex design of reflector of scheffler [18].

In 2010, Munir and others attributed the design principle and fabrication of $9m^2$ surface area of scheffler reflector. The numerical computations to implement reflector parabolic curve and the elliptical reflector positioning regards Equinox through selecting a particular lateral section of paraboloid are recorded. The system is design flexible simplistic and does not need any specific computational system thus allowing a huge inherent of uses in domestic and industrial contours [19].

In 2012, Vishal and others developed, designed and analyzed the enhancement of scheffler reflectors $18m^2$ for 3 bar pressure as 120 degree celsius temperature practically. The setup was deliberated for the hostel of 600 students in Shivaji University that utilizing scheffler technology as low pressure & the temperature steam as well as water heating motive [20].

2.5 The research gaps

Few of researchers constructed composite desiccant through composition of $CaCl_2$ by zeolites, silica gel and clay. Some of them also work on composite desiccant through $CaCl_2$ & jute and saw wood. Composite desiccant is constructed from a combination of $CaCl_2$ and brick granules. Few researchers concentrated for the utilize hot air discharged from fans & blowers which uses the maximum grade energy for resurgence of integrated material of desiccant with evacuated tube of solar air collector, flat plate collector, and the vacuum tube collector of the heat pipe.

Some researchers completed work on resurgence of material the desiccant, utilizing dish of parabola. Resurgence of several state saturated desiccant on the basis of wet such as operated alumina, the silica gel, the molecular sieve, operated charcoal and the novel composite desiccant are transferred to observe the moisture availability by using high generated temperature of secure focus solar concentrator of scheffler at its focal.

2.6 Objectives of the recent work

The overall goal of research is to create a solar powered resurgence system of desiccant. The particular objectives include-

1. To design and create the necessary size of solar concentrator of scheffler for resurgence of the different saturated desiccant.

2. To create a low cost, long lasting, Powered by solar regenerating material of desiccant for the use in dehumidification of air.

3. To compare experimentally the moisture adsorption capacity of several composite and solid desiccant.

4. To create a mathematical analysis of solar drying for the novel composite desiccant.

2.7 Adopted methodology

In the recent work, the adopted methodology is as follows:

1. A thorough review of the literature has been conducted and the research results have been identified.

2. A number of design and operational parameters have been discovered.

3. The solar concentrator of scheffler is fabricated and designed.

4. A new composite desiccant has been developed.

5. After that, the concentrated is utilized for renew the diverse solid and innovative desiccant composite.

6. Furthermore, composite desiccant drying curve is modeled mathematically.

2.8 Conclusion

An extensive literature review was conducted and research results were discovered in this chapter.

3. The designing parameter and mathematical calculation of the solar concentrator of Scheffler

3.1 Introduction

The full mathematical calculations and design of collector frame, crossbars, depth of crossbar of ellipse including design of Scheffler's solar collector have been described in this chapter. This chapter also includes total cost estimation and manufacturing of solar concentrator of scheffer. The design approach adhered to strict design standards and thoroughly examined the relationship between the major systems of the reflector sheets, base, structure and also height from the ground as they were created in tandem. Figure 3.1 depicts a scheffler focus concentrator as the lateral portion of the paraboloid.

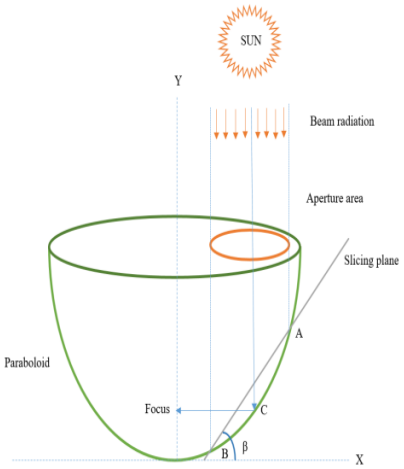

Figure 3.1: Section of the scheffler solar concentrator in a paraboloid.

3.2 Frame of Concentrator

All calculations are made while designing the parabolic curve of the solar concentrator of scheffler made with calculation reference to the equinox. Parabolic curve, all the calculations are made as considering side view of paraboloid with this way, the paraboloid and the concentrator structure are drawn in the shape a parabola curve and also straight line. We could write the normal parabola equations by its axis crossing through the y-axis and the vertex at the source in the following way:

$$x^2 = 4fy \qquad (3.1)$$

Where; f is parabola focal length.

The Equation of line of parabola for slicing plane is,

$$y = mx + c_1 \qquad (3.2)$$

In which; m = slope of line (tan β) and C_1 = y intercept of the line, β = inclination of the slicing plane in sequence to approximately built equilibrium reflector at two points A and B such as AC=BC and reason to select these points are to construct stable parabola in sequence to rotate the reflector by a simple force. Point C is point on the parabola where the falling radiation and the reflected ray produces 90^0 angle by each other and the coordinates are (2f,f).

By this way, line of joining these two points A & B of parabola curve shows the cutting part of elliptical structure of the solar concentrator of scheffler.

Coordinates of points A & B could be calculated by resolving equation (3.1) and (3.2) as follows:

$$x_{A,B=2fm} \pm 2((fm)^2 + fc_1)^{1/2} \quad (3.3)$$

$$y_{A,B=2fm} \pm 2((fm)^2 + fc_1)^{1/2} + c_1 \quad (3.4)$$

Semi major axis (b) of ellipse semi minor axis (a) of the ellipse established by intersection of parabola and also slicing plane could now be deliberated by:

$$a = 0.5(x_a - x_b) \quad (3.5)$$

$$b = 0.5[(x_a - x_b) + (ya - yb)^{1/2} \quad (3.6)$$

All of the expressions are computed and organized in such a way that a solar concentrator of scheffler may be constructed if focus of parabola and area of collector are known.

Table 3.1 shows the results of the current calculations of a collector area of 1.53 m^2 and focus of about 0.571 m. Figure 3.2 depicts the entire details of crossbars on the parabola curve and also scheffler.

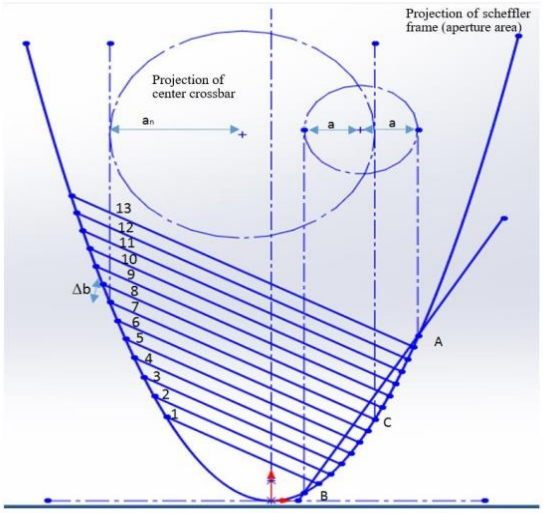

Figure 3.2: Illustration of scheffler and crossbars on parabolic curve.

Table 3.1: Scheffler solar concentrator designing parameter.

Term Specification	Following Dimensions
Parabola's local length (f)	0.581 m.
Slicing plane's slope (m)	0.942m
Slicing place's intercept (C_1)	0.351m
Slicing plane in angle (β) Slope	43.10^0
Semi major axis (b)	0.918 m.
Semi minor axis (a)	0.693m.

3.3. The Crossbars

The correct arrangement of crossbars of frame of reflector is required to the construction of solar concentrator of scheffler. The elliptical form of the solar concentrator of scheffler, frame may be simply determined by utilizing the equation of ellipse, as follows:

$$\frac{x_n^2}{b^2} + \frac{y_n^2}{a^2} = 1 \quad (3.7)$$

In which (a) represents the semi-minor axis and (b) is semi-major axis of the ellipse. For locating any point "Yn" regarding to "Xn" on the frame of ellipse, mentioned equation is again modified as:

$$Yn^2 = (cos\beta)(b^2 - x^{2\,n}) \quad (3.8)$$

Equation is used to determine the location of crossbars of elliptical frame of reflector of the scheffler (3.8). As needed the main axis (2b) is split into multiple sections. Origin is centre of an ellipse, the major axis is along x-axis and it passes from the origin. By plugging the value of Xn into equation (3.8), the value of Yn can be calculated, and therefore the location of the crossbars on the frame of elliptical of scheffler concentrator can be evaluated. The Number of crossbars as 13 is chosen to shape the appropriate part on 1.53 m^2 elliptical frames in such a way that reflector sheet may adopt the requisite form of the concentrator. Figure 3.3 depicts the junction sites on frame of the reflector.

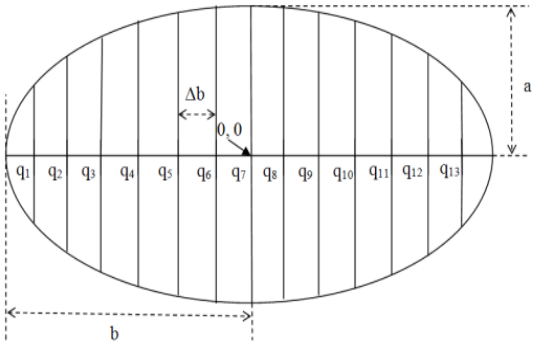

Figure 3.3: The intersection points on the reflector frame of thirteen crossbars ($q_1 - q_{13}$).

Succeeding the fabrication work of reflector frame, crossing points of crossbars are pointed on elliptical frame of reflector for variables evaluated utilized preparation of the needed crossbars of sheffler reflector. The lengths of arcs (b_n) and depth (Δ_n) for thirteen crossbars have been evaluated to fabricate the reflector of scheffler by using trigonometric equations. After all of the dimensions are determined then these crossbars are make ready to form

scheffler reflector and also bolted on mentioned points of reflector frame of scheffler. From these equations, crossbars be prepare to form scheffler reflector and also are bolted on the mentioned points of frame of scheffler reflector to evaluate the correctness of bent crossbars, the design of flex print was employed.

Table 3.2: The position of crossbars on an elliptical frame as measured from center of the ellipse.

Number of crossbars	Xn	Yn
1	-0.703	± 0.309128
2	-0.586	± 0.413879
3	-0.469	± 0.492261
4	-0.352	± 0.541902
5	-0.235	± 0.574737
6	-0.118	± 0.593565
7	0	± 0.593709
8	0.118	± 0.593565
9	0.235	± 0.574737
10	0.352	± 0.541902
11	0.469	± 0.492261
12	0.586	± 0.419879
13	0.703	± 309128

3.4 The depth for the crossbar ellipses and calculation of the equations

Figure 3.2 depicts the cutting planes of crossbars as 13-straight line normal to the cutting plane of frame of reflector. The cutting plane of crossbar has a (90+ β) inclination angle. Cutting lines are likewise ellipses with the same axis ratio ($\frac{a_n}{b_n} = \cos(90 - \beta)$).

Starting at the middle of crossbar (q_7), we extract the basic equation of line and it is given as:

$$y = m_{n^x + c_n} \quad (3.9)$$

In which m_n is slope of the cutting plane, c_n is intercept and n is number of the crossbars. Because all of the cutting planes are parallel, m_n will be constant for all of them. Semi minor axis of the ellipse is determined by using-

$$a_n = 2((f.m_n)^2 + f.c_n)^{1/2} \quad (3.10)$$

The above equation is applicable for central crossbar only, for rest of the crossbars c_n is change by $\pm\Delta b/sin\beta$.

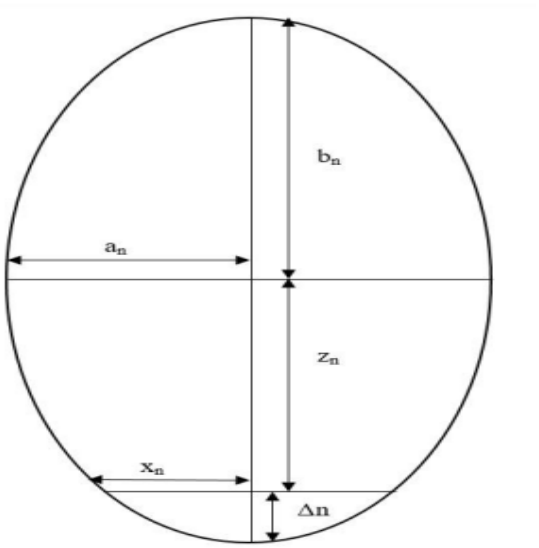

Figure 3.4: Ellipse of crossbar for concentrator of scheffler (SC).

The nth crossbars (Δn), depth of concentrator is calculated by using the equation which has deduced from geometry of an ellipse:

$$z_n = \frac{(a_{n^2 - x_{n^2}})^{1/2}}{COS\,(90-\beta)} \quad (3.11)$$

$$\Delta n = b_n - z_n = \frac{a_n - \left(a_{n^2 - x_{n^2}}\right)^{1/2}}{\cos(90-\beta)} \quad (3.12)$$

3.5 Forming of solar concentrator of scheffler

Working drawings of the frame of reflectors and the crossbars are created using solid works as illustrated in figure 3.5. The drawing was utilized to fabricate the frame of reflector and the crossbars.

Table 3.3: The Semi major and semi minor axes of the elliptical crossbars as well as the depth of several arcs of crossbars are shown.

Number of crossbars	Xn	Yn
1	-0.703	± 0.309128
2	-0.586	± 0.413879
3	-0.469	± 0.492261
4	-0.352	± 0.541902
5	-0.235	± 0.574737
6	-0.118	± 0.593565
7	0	± 0.593709
8	0.118	± 0.593565
9	0.235	± 0.574737
10	0.352	± 0.541902
11	0.469	± 0.492261
12	0.586	± 0.419879
13	0.703	± 309128

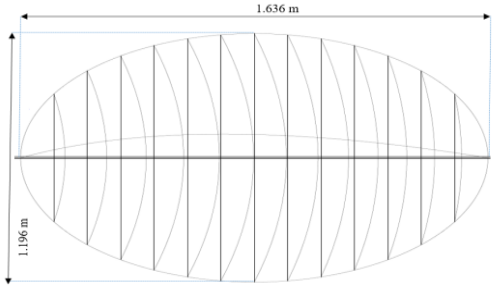

Figure 3.5: The crossbars of the scheffler solar concentrator (SSC) and drawing of solid works for reflector frame.

Reflector frame structure was elliptical in shape as shown in Figure 3.5. It was linked in two parts with bolts and nuts after bending into an elliptical shape. Following the installation of the reflector frame, the centre was bent according to the design and attached to the frame of reflector as illustrated in figure 3.6. They were linked by frame of reflector center bar by the help of bolts and nuts. Anodized sheets of aluminum for reflecting material were used.

Solar concentration of scheffler is a lateral part of a paraboloid and it is designed concerning of equinox (solar declination = 0). To achieve the fixed focus all days, various paraboloid surfaces are required based on solar declination. So that the scheffler reflector is reflector is given by three points. In which two pivot points are attached with a reflector frame while the third is attached to parabola curve. When the reflector is cyclic changed by the help of the telescopic clamp mechanism by revolving at half solar declination angle, these pivoted points induce the needed change in the form of the crossbars. For this purpose the all frame of scheffler reflector is fabricated like flexible assembly to achieve the desired.

Figure 3.6: Construction of reflector frame, the crossbars of the scheffler solar concentrator.

3.6 Total Cost Estimation

Fabrication work of reflector of scheffler was completed in Gorakhpur. All cutting, fitting, drilling and assembly procedures for reflector of scheffler were completed at my own place Gorakhpur in a private workshop. Table 3.4 shows an estimate of the total cost in rupees.

Table 3.4: Total Cost

Item	Cost (Rs.)
Frame of reflector	1800
The Structural stand	2200
Mechanism for Tracking	600
Bolts and Nuts	600
Printing Flex	400
Labor charge	1100
Total Cost Rs.	6700

All of the necessary tools and equipments were accessible at the private mechanical workshop to perform all the procedures.

The majority of the work was cold with some welding thrown in for good measure. As a result the first cost incurred in the manufacturing of the solar concentrator of scheffler, was material cost.

3.7 Conclusion

All of the calculations are made while creating parabolic curve of solar concentration of scheffler made with reference to equinox. All of the expressions are computed and organized in such a way that the solar concentrator of Scheffler may be constructed if focus of parabola as well area of collector is known. The present estimate is done to a collector of area 1.53m^2 and focus distance of 0.571m. The correct arrangement of crossbar of reflector frame is required to the fabrication of scheffler collector. As a reflective medium, anodized aluminum sheets were utilized. To ensure that the correctness of bent crossbars a

new flex print of design sketches was employed. Various paraboloid surfaces are required to achieve the same focus. The reflector of scheffler has 3 points for this aim, reflectors frame is attached with 2 pivot points and the third is attached to the centre of bar (parabola curve) These pivoting procedures the needed change in form of crossbars when reflector is adjusted seasonally, using the mechanism of telescopic clamp by moving at partial the solar of declination angle.

4. Experimental difference of the various solid & desiccants composite for resurgence through the scheffler solar concentrator (SSC).

4.1 Introduction

This chapter comprises the information of experimental system installed at my place Gorakhpur India 26^0 77^1 North and $83^0 37^1$ East) together with computing instruments and devices, setup operation and practical uncertainly. The practical were managed in the month of March. The experiments were organized on the saturated desiccants to detect maximum adsorption value of several desiccants i.e. molecular sieve, silica gel, alumina, operated charcoal, and novel desiccant composite.

4.2 Experimental Setup

The experimental setup utilized for evaluation of moisture availability in several saturated desiccants as illustrated in the Figure 4.1.The investigation was conveyed at SIIT Gorakhpur India $83^0 37^1$ and East26^0 77^1 North). Saturated sample of 0.60kg is selected to the research of the every desiccant resurgence is conveyed from removing the desiccant to direct heat, given by the concentrator of solar at fixed focus.

(a) **(b)**

Figure 4.1: Pictorial view of the experimental setup from (a) front view (b) side view, which is utilized for resurgence of many material of desiccant.

Complete practical system is made up of following components which are labeled as:

i. Solar concentrator of scheffler (SSC.)

ii. Receiver

4.2.1 The solar concentrator of Scheffler (SSC).

An area of 1.53 m^2 SSC is utilized for the accumulation radiation of solar for the desiccant infused in the receiver. The sheet of anodized aluminum utilized as an accumulator material. Setup of solar concentrator has installed at Gorakhpur (an angle balance to the latitude of the detection, facing towards south for greatest utilization of concentrator). The solar tracking has been completed after the gap of 10 minutes. A graphic concentrator diagram is illustrated in figure 4.2.

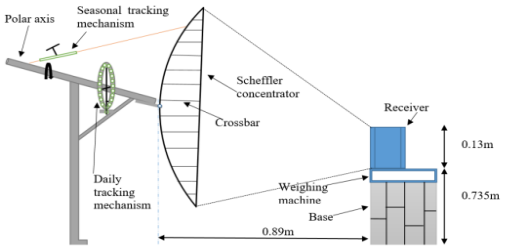

Figure 4.2: Simplified diagram of scheffler solar concentrator (SSC).

4.2.2 Receiver

The container of receiver is exposed of metal sheet and is 0.13m x 0.11m x 0.05m in size. The rear and front sides of the receivers are sheltered with mesh to contain the desiccant, and few holes are supplied on the perimeter to moisture extraction.

(a) (b) (c) Figure 4.3(a)Simplified representation of the receiver from (b) front view (c) side view.

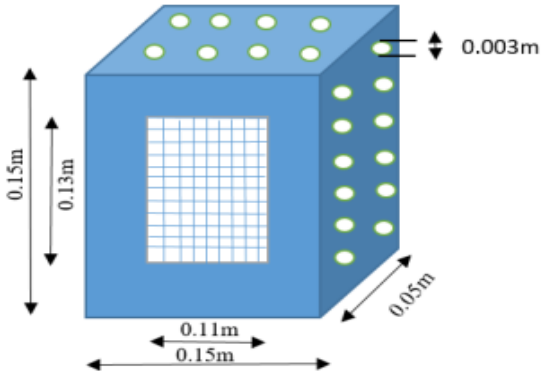

Figure 4.4: Graphic diagram of the receiver.

4.3 Operation of the system

System is utilized for focus the radiation of solar at a point of focus. A receiver infused with the desiccant of material, is set on its focus for regenerating material of desiccant through utilizing physical heat given by setup. The receiver is merged with the weighing machine for lookout, the loss in weight of material of desiccant after the each 10 minutes of gap. Tracking of sun in the day is completed at each 10 minutes of gap by the use of holes drilled above the polar axis of concentrator on the ring. Focused radiations enhance temperature of desiccant surface. Surface temperature of desiccant material enhances difference in desiccant pressure of vapor and atmospheric air enhances as a outcome of moisture from desiccant Surface, start removing.

Practical examination, data on the surface temperature, the weight loss, WBT & DBT, the solar intensity and wind speed of several anhydrous materials are found. Resurgence rate and the moisture availability of its saturated sample of several desiccants (wet) are estimated. The resurgence of material of desiccant is quantity of moisture extracted by desiccant in per unit time as illustrated in figure 4.1.

Where; Resurgence rate (kg/hr) = $m_{desiccant}$ (4.1)

In which; mdessicant is mass of desiccant (dry basis), d_w shows the change in desiccant weight, and the d_t shows time gap when change is examined [7]. Dry basis Availability can be found by using the equation shown in (4.2). It is the ratio of mass of the H_2O in desiccant to mass of desiccant (dry).

$$MC\ (kg/kg) = \frac{m_w - m_d}{m_d} \quad (4.2)$$

In which; m_w shows mass desiccant (kg) (wet), and m_d is mass desiccant (kg) (dry).

4.4 Instruments and measuring device

Instruments and the devices used for practical investigation are as follows:

I. The intensity of Solar is calculated with a pyranometer by an accuracy measurement of $\pm 1 W/m^2$.

ii. Sling psychrometer is used to test the DBT and WBT of atmospheric air.

iii. Resurgence rate is found by weighing the material at a gap of 10 minutes.

iv. The thermocouple combine with the help of digital indicator by a least count (0.1^0C), is applicable for measuring desiccant material surface temperature.

v. An anemometer is utilized to measure the wind speed during experimentation with an accuracy of $\pm 0.1 m/s$.

4.5 Experimental Variability

The variability and errors or mistakes in experiments can rise for a variety of reasons which includes calibration, atmospheric conditions, observations, wind speed, test preparation, readings and instrument selection. In this study the suitable best equipment are utilized to assess the losses of weight, DBT & WBT, sun's radiation, and the temperature.

If the variability in all of the independent variables is supplied with the same odds [21], the resulting variability is computed using the expression equation (4.3).

$$w_r = \{ \left[\frac{\partial R}{\partial x_1} w_1\right]^2 + \left(\frac{\partial R}{\partial x_2} w_2\right)^2 + \ldots + \left(\frac{\partial R}{\partial x_n} w_n\right)^2 \}^{1/2} \quad (4.3)$$

In which; w_1, w_2, w_3, ..., W_n is the variability in independent variable and W_R is total variability in results. R is the given function of independent variables X_1, X_2, X_3... X_n.

The variability in the measurements of temperature (w_T) increases by digital thermometer, thermocouples, and value of intersection points. Total variability in measurement of temperature is estimated as:

W_T = [(W thermometer) ^{2} + (W digital thermometer) ^{2} + (W connection points) ^{2} + (W readings) ^{2}]$^{1/2}$

$$W_T = [(0.251)^2 + (0.10)^2 + (0.10)^2 + (0.251)^2]^{1/2} = 0.381.$$

The variability in loss of the weight measurements (w_g) increases by anemometer, values and air leaking. Variability in loss of weight measurements are found as:

$W_g = [(W_{\text{digital weighting machine}})^2 + (W \text{ friction})^2 + (W \text{ readings})^2]^{1/2}$

$W_g = [(1.0)^2 + (0.51)^2 + (1.0)^2]^{½} = 1.502$

The variability in speed of the wind measurements (w_v) increases by anemometer readings and air leaking. Total variability in speed of wind measurements is found as:

$Wv = [(W \text{ anemometer})^2 (W \text{ leaking})^2 + (W \text{ readings})^2]^{1/2}$

$Wv = [(0.10)^2 + (0.10)^2 + (0.10)^2 + (0.101)^2]^{½} = 0.171$

The variability in reading of the WBT (W_{WBT}) &DBT (W_{DBT}) using sling psychrometer (Wv) increases by thermometer. Total variability in WBT &DBT measurements is evaluated as:

$W_{DBT} = W_{WBT} = [(W \text{ thermometer})^2 + (W \text{ readings})^2]^{1/2}$

$W_{DBT} = W_{WBT} = [(0.101)^2 + (0.102)^2]^{½} = 0.142$

The variability from calculation of the solar energy (W_{Se}), increased by pyranometer. Total variable in energy of solar calculations is estimated as:

$Wse = [(W \text{ pyranometer})^2 + (W \text{ readings})^2]^{1/2}$

$Wse = [(1.01)^2 + (1.02)^2]^{½} = 1.142$

Table 4.1: Uncertainty in values during experiment.

Parameters of Corresponding	Units	Comments
Variability in temperature measurements	^{0}C	±0.381
Variability in DBT measurement	^{0}C	±0.142
Variability in WBT measurement	^{0}C	±0.142
Variability in measurements of weight loss	G	±1.502
Variability in measurements of wind speed	m/s	±0.171
Variability in solar energy measurement	w/m^2	±1.415

4.6 Discussions and the experimental results

The investigational procedure is focused on resurgence of the solid desiccants saturated in search to got availability in desiccants utilizing system having an area of 1.53m^2.

The desiccant resurgence is depends on desiccant surface temperature and wind speed. The procedure of practical inspection is same for all the 5 cases; only the variation is differing in the material corresponding to resurgence.

Case-1: Silica gel resurgence

0.60 kg weight of Silica gel is filled in receiver and pointed focus of the system. Between the researches the humidity ratio of air falls between 0.008618-0.011079 kg of water vapor/kg of dry air which has no impact on silica gel resurgence. Silica gel regenerating research, few values are sustained during methods as illustrated in table 4.2.

The impact solar intensity and speed of wind over the silica gel temperature is represented in figure 4.5 & figure 4.6 respectively. Silica gel surface temperature enhances with enhance in the solar intensity, yet wind speed has impacts on it also. The intensity of solar is maximum (12.35 PM i.e. 918w/m^2) but at the parallel time wind speed is high (3.0m/s, which outcomes into a temperature of 90.6^{0}C. Highest temperature of 169.7^{0}C is gained at 01.25 PM while the wind speed and solar intensity is 0.5m/s and 860w/m^2. This represents that wind speed has a remarkable impact on surface temperature desiccant material. The of resurgence rate with time, silica gel surface temperature is illustrated in figure 4.7. This rate of resurgence is high at first due to the more availability of the silica gel but it gradually diminishes.

Table 4.2: Data on solar intensity, wind speed, desiccant (silica gel) weight, silica gel surface temperature and DBT & WBT of atmospheric air are collected every 10 minutes.

Time in hour	Weight of the desiccant in (kg)	Resurgence rate in (kg/hr)	Intensity of Solar in (w/m^2)	Temp. of Surface (°C)	Wind Speed (m/s)	DBT (°C)	WBT (°C)	Humidity ratio of Air
11:35	0.600	-	849	20.6	1.41	19.1	15.51	0.009650
11:45	0.609	0.035	869	83.8	1.52	19.6	16.01	0.009444
11:55	0.592	0.032	886	108.2	1.35	21.6	16.52	0.009185
12:05	0.582	0.029	893	111.4	1.12	20.6	16.01	0.010179
12:15	0.579	0.029	893	96	1.35	21.1	15.51	0.009392
12:25	0.565	0.021	863	86.9	2.01	21.6	16.02	0.008618
12:35	0.55	0.041	918	90.6	3.00	21.0	15.50	0.009292
12:45	0.54	0.047	864	91.0	0.41	21.1	16.51	0.009972
12:55	0.52	0.045	861	97.6	2.23	21.1	16.01	0.009392
13:05	0.521	0.012	855	121.5	0.51	21.1	16.01	0.009392
13:15	0.505	0.030	863	119.5	0.50	22.00	16.00	0.009379
13:25	0.498	0.025	864	169.7	0.50	22.00	16.00	0.009979
13:45	0.496	0.015	802	114	1.61	23.1	16.51	0.009145
13:55	0.492	0.012	785	113.1	0.61	22.1	16.02	0.008979
14:05	0.480	0.009	817	147	0.41	20.6	15.51	0.009030
14:15	0.480	0.0000	801	122.7	0.52	24.1	17.01	0.009322

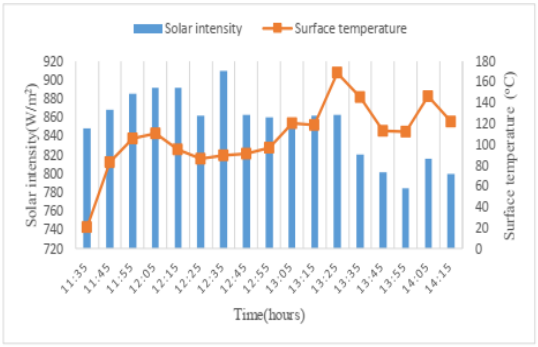

Figure 4.5: Difference in temperature of surface for the solar intensity throughout the silica gel resurgence.

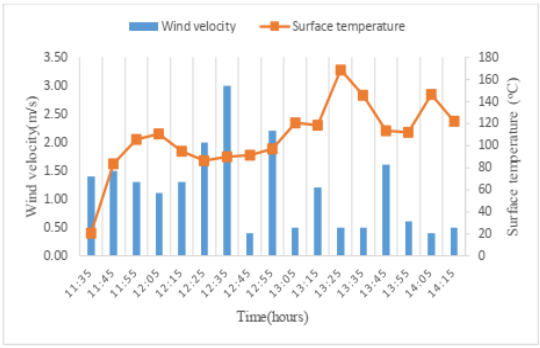

Figure 4.6: Result of wind speed on temperature of the surface throughout the silica gel resurgence

The highest temperature of about 169.7^{0}C is gained at 01:25 PM when the intensity of solar is 860w/m^2 and wind speed is 0.5m/s, this represents that speed of wind has a remarkable impact on temperature of desiccant material surface. The fluctuation rate of resurgence with time, the silica gel surface temperature is illustrated in Figure 4.7. The rate of resurgence is high at first due to the more availability of silica gel, and it is gradually decreases as the time passes.

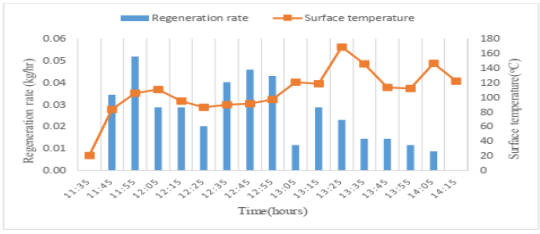

Figure 4.7: The difference in the resurgence rate of the new composite of silica gel with temperature of surface is demonstrated throughout a 10 minutes time gap.

The investigation's findings are described below:

i. The highest rate of resurgence of 0.0520kg/hr is gained at "Ts" of 106 ^{0}C.
ii. Average wind speed average surface temperature and average solar intensity throughout the investigations are 1.08m/s, 108.30^{0}C and 852.76w/m^2 respectively.
iii. The highest temperature of 169.7^{0}C is gained at silica gel at wind speed of 0.5m/s.
iv. Figure 8 depicts the color shift of the silica gel from pink to blue as a sign of full resurgence.
v. Under these conditions, full resurgence of silica gel get hold of 160 minutes and weight decreases of 22.751 percent is obtained.

Silica gel has a moisture availability of 0.2945 kg of water per kg of dry desiccant.

(a) (b)

Figure 4.8: Real pictorial representation of silica gel in receiver which is positioned above the weighing machine at (a) after 20 minutes, and (b) after 140 minutes of the resurgence.

Case-2: Operated alumina resurgence

In this case 2, 0.60 kg of operated alumina is put into the receiver and positioned at the SSC's focus. Throughout the research; the humidity ratio ranged from 0.00721 to 0.11985 kg of water vapor/kg of dry air, which had no influence on operated alumina resurgence. Few readings are taken throughout the resurgence research of the operated alumina as indicated in Table 4.3.

Table 4.3: The data on solar intensity, wind speed, desiccant operated alumina weight, temperature of surface of operated alumina and DBT & WBT of atmospheric air are collected every 10 minutes.

Time in hour	Weight of the desiccant in (kg)	Resurgence rate in (kg/hr)	Intensity of Solar in (w/m^2)	Temp. of Surface (°C)	Wind Speed (m/s)	DBT (°C)	WBT (°C)	Humidity ratio of Air
14:30	0.60	-	755	27	0.7	26.1	16.6	0.007811
14:40	0.625	0.0175	707	123.0	1.1	22.1	14.7	0.007210
14:50	0.616	0.0316	616	112.6	1.7	21.6	14.6	0.007416
15:00	0.610	0.0210	610	95.3	1.4	22.6	15.6	0.008116
15:10	0.602	0.0269	615	76.6	1.82	22.1	15.7	0.008313
15:20	0.599	0.0115	727	129.1	0.52	22.1	15.6	0.008313
15:30	0.594	0.0184	667	103.6	0.41	23.1	15.6	0.007910
15:40	0.584	0.0045	583	119.2	0.72	21.1	15.7	0.008734
15:50	0.582	0.0079	521	93.6	1.21	22.1	16.2	0.008889
16:00	0.582	0.0000	446	88.6	1.42	22.1	18.6	0.011995

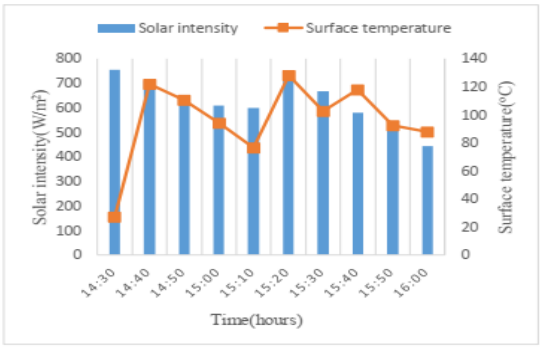

Figure 4.9: Throughout the resurgence of operated alumina, the fluctuation of surface temperature with sun intensity is shown.

Figure 4.9 and 4.10 depicts the influence of wind speed of operated alumina, surface temperature and intensity of solar. At 03:10 PM, the sun intensity is 615w/m^2 and the speed of wind is 1.82m/s, resulting in temperature of a surface of 76.6^{0}C for operated alumina. However at 03:40 PM, the wind speed and solar intensity are 0.72m/s and 583w/m^2, respectively resulting in a Ts of 119.2^{0}C demonstrating the influence of wind speed on desiccant material surface temperature.

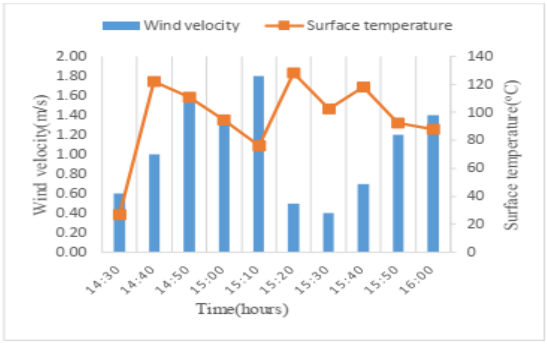

Figure 4.10: The outcome of wind speed on temperature of surface throughout the resurgence of operated alumina.

Fluctuation rate of the resurgence with time period of the surface temperature of operated alumina is illustrated in figure 4.11. When compared to example 1, the resurgence time of operated alumina is relatively short (silica gel).

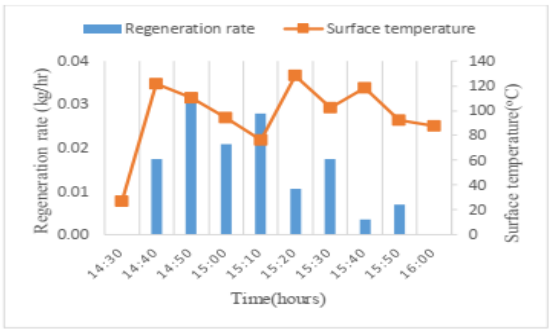

Figure 4.11: Variation of operated alumina resurgence, rate as a function of surface temperature is displayed once every 10 minutes.

The followings are the findings of the investigations.

i. The highest rate of resurgence is 0.0316kg/hr attained at the surface temperature of 112.6^{0}C.

ii. Solar intensity average, average wind speed and average surface temperature throughout the investigations are 624.8w/m^2, 1.1m/s and 96.86^{0}C respectively. Because of the decreased sun intensity throughout the research, “Ts” was observed to be lower than in instance 1.

iii. The highest temperature as of 129.1^{0}C is attained on surface of operated alumina corresponding the speed of wind is 0.52m/s which are lower compared to the highest temperature attained as case1, in spite of likely same speed of wind as of less intensity of solar throughout the inspection.

iv. Under the circumstances, full resurgence the operated alumina get hold of 90 minutes and weight decreases of 6.30 percent is obtained.

v. In comparison to instance 1, the moisture availability of operated alumina is 0.0672kg of water per kg of dry desiccant (silica gel).

Figure 4.11 (a) shows the white fused alumina.

Figure 4.11 (b) shows the silica gel.

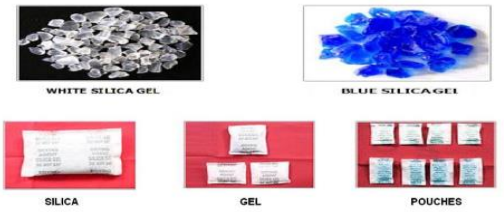

Figure 4.11 (c) shows the type of silica gel.

The conclusion represents that adsorption potential of the silica gel is far higher when compared to operated alumina.

Case-3: Molecular strainer resurgence

In this put down molecular strain consisting weight of 0.60kg is placed in receiver and put down at the focus of system throughout examination, humidity ratio of air falls between 0.008161-0.01112 kg of water vapor/ kg of dry air which has no significant on resurgence of the molecular strain. For the resurgence, examination of molecular strain several values are found during investigation as illustrated in Table 4.4.

Table 4.4: Data on solar intensity, wind speed, desiccant molecular weight, temperature of surface of the molecular sieve and DBT & WBT of atmospheric air collected every 10 minutes.

Time in hour	Weight of the desiccant in (kg)	Resurgence rate in (kg/hr)	Intensity of Solar in (w/m^2)	Temp. of Surface (°C)	Wind Speed (m/s)	DBT (°C)	WBT (°C)	Humidity ratio of Air
10:50	0.600	-	670	19.91	0.92	19.2	15.1	0.008998
11:00	0.613	0.0253	685	136.21	1.31	19.6	15.6	0.009345
11:10	0.608	0.0162	749	156.1	0.51	21.1	15.6	0.008824
11:20	0.604	0.0131	744	160.12	1.32	21.6	15.1	0.008161
11:30	0.591	0.0306	781	138.78	0.51	21.1	15.1	0.008266
11:40	0.585	0.0193	784	153	1.50	20.1	16.2	0.009806
11:50	0.573	0.0375	0.0375	801	154.91	0.42	22.2	0.008412
12:00	0.565	0.0254	803	193.31	0.42	19.2	15.6	0.009650
12:10	0.553	0.0375	786	152.12	0.42	20.1	16.1	0.009805
12:20	0.551	0.0071	671	151.68	1.01	19.2	16.2	0.011120
12:30	0.541	0.0315	816	194.34	0.52	21.2	16.1	0.009293
12:40	0.530	0.0345	790	180.3	0.42	21.1	16.1	0.009293
12:50	0.516	0.0428	785	188.4	0.42	21.6	16.8	0.009091
13:00	0.509	0.0223	778	188.3	0.42	22.2	16.8	0.009443
13:10	0.509	0.0000	767	142.34	1.12	23.2	16.2	0.008824

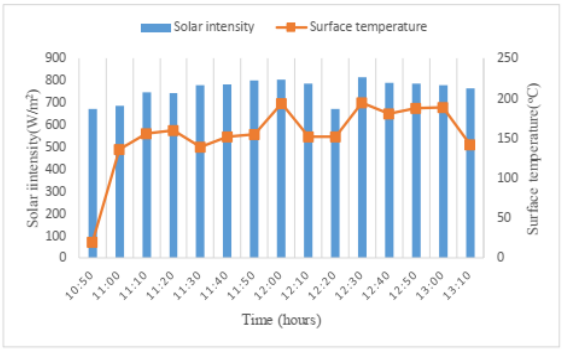

Figure 4.12: The graph depicts the variation of temperature of surface with the intensity of solar. Figure 4.13: During resurgence, the impact of wind speed on the surface temperature. throughout resurgence of molecular sieve.

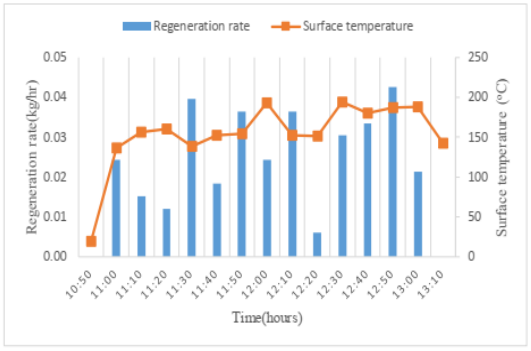

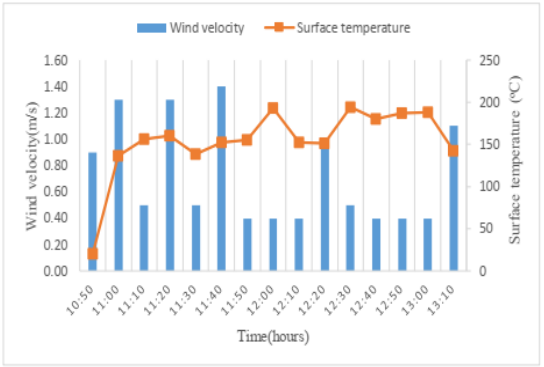

Figure 4.14: The difference in molecular sieve rate of resurgence with temperature of surface is shown of a time gap of 10 minutes.

The experimentations findings are as follows:

i. The greatest rate of resurgence is 0.0428kg/hr is attained at surface temperature of about 188.4^{0}C.

ii. Solar intensity average, average wind speed and the average surface temperature throughout the experiments are 760.73w/m^2 0.7493m/sec and 153.98^{0}C respectively. Suggested that the average surface temperature throughout the investigation is more as of less speed of wind and best sun's intensity throughout the investigation.

iii. The highest temperature of surface of about 194.34^{0}C is attained at the of molecular strain surface as the speed of wind is 0.42m/s.

iv. It gets hold of 140 minutes in total resurgence of molecular strain below corresponding situations, and loss of weight of about 18.074% is attained. Loss in weight is little lower compared as attained in case 1, yet more compared as in case 2.

Moisture level of strain of molecule is of 0.2215kg of water per kg of dry desiccant, which is equivalent as in case 1(silica gel). The outcomes reveal that molecular strain (size) has a greater adsorption potential than the silica gel, although it needed a greater temperature of resurgence.

Case-4: Operated charcoal resurgence

In this stage operated charcoal weighing 0.60kg is put on in the receiver. Throughout the research, the humidity ratio of air ranged in 0.008763 & 0.012435kg of water per kg of the dry air, which had no significant on operated charcoal resurgence. Multiple readings are taken throughout the resurgence research of operated charcoal as indicated in Table 4.5.

Table 4.5: Data on solar intensity wind desiccant activated charcoal weight speed, temperature of surface of operated charcoal and DBT & DBT of atmospheric air are collected every 10 minutes.

Time in hour	Weight of the desiccant in (kg)	Resurgence rate in (kg/hr)	Intensity of Solar in (w/m^2)	Temp. of Surface (°C)	Wind Speed (m/s)	DBT (°C)	WBT (°C)	Humidity ratio of Air
11:20	0.60	-	849	20.42	1.42	21.5	16.3	0.0089
11:30	0.618	0.0104	869	83.15	1.56	20.1	16.4	0.0098
11:40	0.61	0.0281	886	105.62	1.37	21.2	16.6	0.0093
11:50	0.605	0.0175	893	110.41	1.12	21.6	16.2	0.0091
12:00	0.58	0.0175	893	96	1.36	21.6	17.3	0.0103
12:10	0.587	0.0060	863	85.8	2.1	22.6	16.8	0.0087
12:20	0.597	0.0036	912	90.1	3.2	21.2	15.6	0.0088
12:30	0.595	0.0060	864	91.8	0.42	21.6	16.6	0.0097
12:40	0.593	0.0060	861	97.23	2.23	22.6	18.2	0.0120
12:50	0.591	0.0106	855	120.56	0.56	21.6	18.1	0.0124
12:00	0.587	0.0036	863	118.57	1.23	21.2	17.6	0.0120
13:10	0.586	0.0080	864	129.2	1.1	21.6	16.6	0.0097
13:20	0.586	00000	821	115.8	1.52	21.6	17.3	0.0112

Figure 4.15 and 4.16 demonstrated the influence of wind speed and intensity of solar on the new composite surface temperature. The operated alumna's surface temperature rises as the sun's intensity rises, yet it has an impact as well on wind speed. The highest intensity of solar radiation is 912w/m^2 at 12:20 PM, yet the speed of wind is 3.2m/s, resulting the surface temperature is 90.1^{0}C.

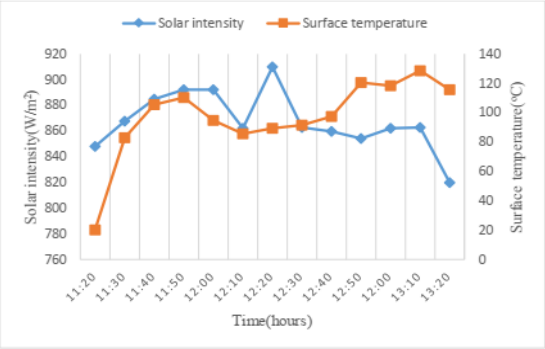

Figure 4.15: The graph depicts the variation in temperature of surface with intensity of solar throughout operated charcoal resurgence.

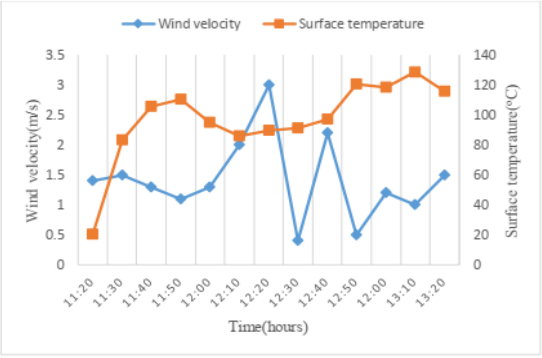

Figure 4.16: The impact of wind speed on surface temperature throughout operated charcoal resurgence.

The highest temperature of 129.2^{0}C is obtained at 01:10 PM when the intensity of the sun and speed of wind are 964w/m^2 and 1.1m/s respectively; demonstrating wind speed has a substantial influence on desiccant material

surface temperature. Figure 4.17 depicts the rate of change of the resurgence with surface temperature of operated charcoal and with time.

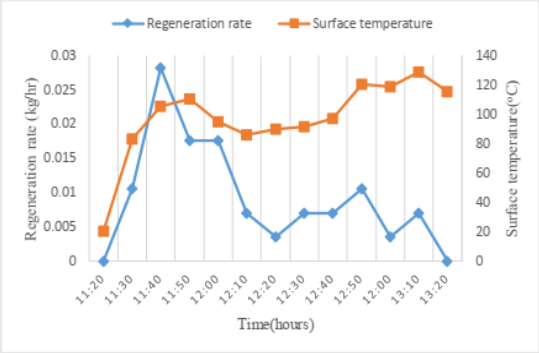

Figure 4.17: The fluctuation of operated charcoal resurgence rate with surface temperature is shown over a time gap of 10 minutes.

The research's findings are as follows:

i. At 105.62^{0}C surface temperature the highest rate of resurgence i.e. 0.0281kg/hr is achieved.

ii. The average intensity of solar, average surface temperature and average wind speed during inspection are 868.69w/m^2, 84.31^{0}C and 1.2793m/s respectively.

iii. When the wind speed is about 1.1m/s, the surface of operated charcoal reaches at highest temperature of 129.2^{0}C.

iv. Under these conditions, the operated charcoal consumes time of 120 minutes for full resurgence, and weight decreases up to 5.29% is obtained.

v. Operated charcoal has a moisture availability of 0.0559kg of water per kg of dry desiccant.

The searches indicate as operated charcoal has a low adsorption capability.

Case-5: Novel composite resurgence

In this study a new composite weighing 0.60kg is loaded in the receiver and put at the focal point of the solar concentrator of scheffler. Novel composite is created by immersing the brick fragments in the 41% $CaCl_2$ and allowing them to absorb availability from the surrounding air, until it saturated. Throughout the research the humidity ratio of air ranged between the 0.009785 and 0.012256 kg of water vapor/kg of dry air, which had no influence on the new composite resurgence. Few readings are taken throughout the resurgence, investigation of new composite material as indicated in Table 4.6.

Table 4.6: Data on solar intensity of wind speed, a novel composite desiccant weight, temperature of surface of a novel composite and DBT & WBT of atmospheric air are collected every 10 minutes.

Time in hour	Weight of the desiccant in (kg)	Resurgence rate in (kg/hr)	Intensity of Solar in (w/m^2)	Temp. of Surface (°C)	Wind Speed (m/s)	DBT (°C)	WBT (°C)	Humidity ratio of Air
10:45	0.600	-	708	20.4	0.53	18.53	15.08	0.009289
10:55	0.608	0.0353	708	71.8	0.91	19.52	15.09	0.009785
11:05	0.559	0.0322	728	78.1	0.82	19.01	15.06	0.009819
11:15	0.599	0.0322	767	100.4	0.84	20.02	15.57	0.009273
11:25	0.589	0.0322	798	71.8	2.23	21.03	16.03	0.009329
11:35	0.569	0.0631	825	112.6	1.86	21.50	16.03	0.009168
11:45	0.564	0.0166	836	124.6	0.89	21.51	16.04	0.009168
11:55	0.551	0.0416	843	104.6	0.92	22.01	17.03	0.011049
12:05	0.549	0.0072	861	103.2	1.67	22.03	16.58	0.009595
12:15	0.539	0.0322	874	88.8	1.01	22.03	17.02	0.011049
12:25	0.531	0.0260	855	76.5	1.92	22.03	17.51	0.012256
12:35	0.531	0.0000	871	118.8	0.44	22.02	17.06	0.011049

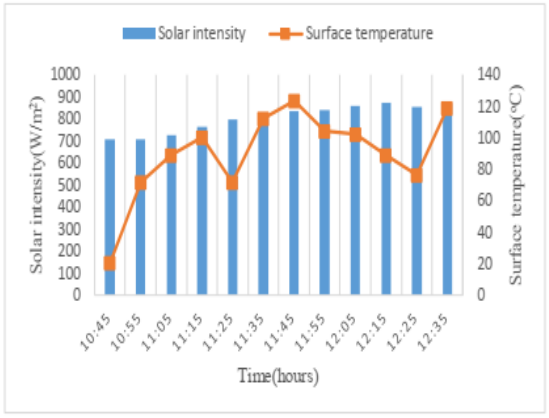

Figure 4.18: The fluctuation in temperature of surface with intensity of solar throughout the resurgence of a novel composite is shown.

Figure of 4.18 and 4.19 depicts the influence of wind speed and intensity of solar radiation on the new composite's surface temperature. The temperature of surface of new desiccant rises as sun intensity rises, yet the speed of wind has also an influence on it. The highest intensity of solar radiation is 861w/m^2 at 12:05 AM, but the speed of the wind is 1.67m/s, resulting in a temperature of surface of 103.2^{0}C.

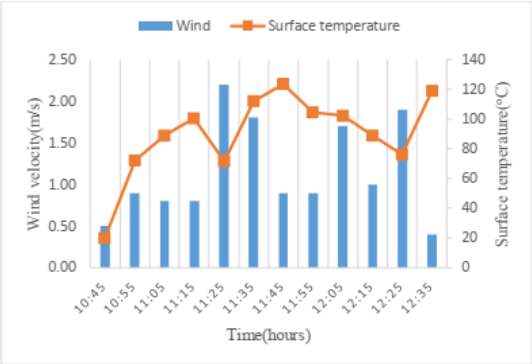

Figure 4.19: The impact of the wind speed on the temperature of surface of a novel composite throughout resurgence.

At 11:45 Am, the highest temperature of 124.6^{0}C is reached when the intensity of sun and speed of wind are 836w/m^2 and 0.89m/s respectively, indicating speed of wind has a substantial influence on desiccant material's surface temperature. Figure 4.20 depicts the change of rate of resurgence with surface temperature and time of new composite material. The rate of resurgence attained in the new composite material is greatest amount of all the possible scenarios.

The consideration's results are as follows:

i. At a temperature of surface of 124.6^{0}C, the highest rate of resurgence of 0.0631kg/hr is attained.

ii. Throughout the experiment, the average intensity of solar, average wind speed and average temperature of surface were 806.33w/m^2, 1.238m/s and 90.2167^{0}C respectively. It is discovered that the average temperature of surface throughout the research is low as a result of the investigation as there was an increases in the wind speed.

iii. When the speed of wind is 0.89m/s, the temperature of surface of desiccant reaches at highest as of 124.6^{0}C.

iv. Under corresponding circumstances full resurgence of new composite takes 110 minutes and there is a decrease in weight of 14.98% is obtained.

Novel composite has a moisture level of 0.18 kg of water/kg of the dry desiccant, in which it is somewhat less compared to instance 1(silica gel) & instance 3(molecular sieve).

Results demonstrate as the new composite has high adsorption availability, similar to traditional desiccant materials because of silica gel and the molecular sieve.

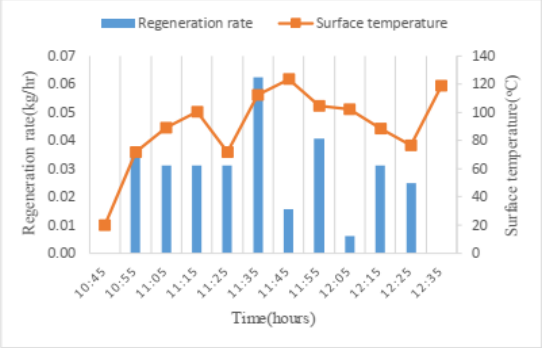

Figure 4.20: The rate of resurgence of a novel composite varies with temperature of surface over a time gap of 10 minutes.

4.7 Conclusion

The temperature of surface, which is affected by intensity of sun and speed of wind influences resurgence of desiccant via direct heat produced by a solar concentrator of scheffler. If the resurgence is executed using direct heat by a solar concentrator of scheffler, the humidity ratio of air has no influence on resurgence of desiccant. Because Silica gel having highest adsorption capacity of any desiccant studied, it is the best desiccant for utilize in building air dehumidification as well as air conditioning system. Because of its moisture availability (less as compared to silica gels) having short resurgence time, the novel desiccant is viable replacement for traditional desiccant.

Moisture availability in operated alumina, silica gel, operated charcoal; molecular sieve and new composite sample of equal weight of various saturated desiccants (on the basis of wet) are 0.0672, 0.2945, 0.0057, 0.2335 & 0.18 kg of water per kg of the dry desiccant respectively.

The operated alumina, the silica gel, the molecular sieve and the new composite desiccants had the times of resurgence are 90, 160,140 and 110 minutes, respectively. Figure 4.21 depicts a photographic image of all regenerated materials of desiccant employing 1.53m^2 SSC and the Table 4.6 provides a tabular form of the results achieved in different materials of desiccant. The greatest temperature of surface is 194^{0}C reached in case of resurgence of the molecular sieve by 1.53m^2 solar concentrator of scheffler and highest rate of resurgence is

achieved in new desiccant composite in all the cases which is 0.07440kg/hr.

Figure 4.21: Photographic representation of the SSC resurgence.

Table 4.7: The highest rate of resurgence, loss of weight in percentage, moisture availability (on the basis of dry), range of temperature, range of average temperature, wind speed range, range of average wind speed, range of humidity ratio, data of the solar radiation, range of intensity, and period of resurgence, different desiccant material were obtained by utilizing a 1.53m^2 scheffler solar panel concentrator.

Desiccant composite	The silica gel	Operated alumina	The molecular strain	Operated charcoal	Novel Composite
Resurgence count (kg/hr)	0.0516	0.031	0.0428	0.029	0.0628
loss of weight (%)	22.740	6.28	18.05	5.23	15.998
Moisture availability (on dry basis)	0.2945	0.0672	0.2235	0.057	0.18
Range of Temperature of surface (^{0} C)	20.6-168.8	26.0-128.12	19.7-194	20.6 - 128.9	20.8-123.8
Average temperature (^{0}C)	107.35	95.93	152.70	96.071	88.97
range of wind speed (m/s)	0.5-3.1	0.3-1.9	0.3-1.2	0.3-3.1	0.4-2.3
Wind speed average (m/s)	1.187	1.07	0.78	1.426	1.25
Humidity ratio (kg w.v./kg d.a.) range	0.008519-0.010078	0.007200-0.011899	0.007861-0.010130	0.008873-0.011875	0.008885-0.010852
Range of Solar intensity (W/m^2)	786-918	446-756	678-816	830-920	708-875
Solar intensity Average (W/m^2)	857.78	623.30	769.73	877.62	806.09
Resurgence time (minutes)	160	90	140	120	110

5. The drying curve for the mathematical model of desiccant composite

5.1 Introduction

Drying curve for desiccant composite has been modeled mathematically in this chapter. For choosing the optimum illustrative model of the drying desiccant composite 12 drying models were incorporated for the practical data utilizing MATLAB tool as the analysis for statistical.

5.2 Analytical model

The data of moisture ratio is transformed to the usable moisture ratio (dimensionless term), and the calculations for curve suited for drying models, furnished from many researchers by the drying period are performed.

Throughout the resurgence, the ratio of moisture of the composite material desiccant is determined by the following equations:

$$MR = \frac{M_t - M_e}{M_0 - M_e} \quad (5.1)$$

In which Mt represents the content of moisture (on basis of dry) at time t, Mo represents the content of moisture (on basis of dry) at time t=0, & Me represents the availability of moisture on stability stage (on basis of dry). Because Me is relatively little in comparison to the original content of moisture, the MR equation is again reduced to Mt / Mo [22]. The expression provided can be used to evaluate the content of moisture on the basis of dry in equation (4.2).

12 alternative models of moisture ratio are suited with research outputs for explaining the drying of desiccant composite, determining the best model by utilizing a solar concentrator of Scheffler, as illustrated in Table 5.1. For regression analysis, the MATLAB software is utilized. Correlation coefficient (R), is key factor for choosing the optimal equation of drying. Another approach for determining the quality of fit is the root average square of error analysis (RSME). For better the match, more the value of R and less as compared to the RSME [23].

$$R^2 = \frac{\sum_{i=1}^{n}(MR_i - MR_{pre,i}).\sum_{i=1}^{n}(MR_i - MR_{exp,i})}{\sqrt{\left[\sum_{i=1}^{n}(MR_i - MR_{pre,i})^2\right].\left[\sum_{i=1}^{n}(MR_i - MR_{exp,i})^2\right]}} \quad (5.2)$$

$$RMSE = \left[\frac{\sum_{i=1}^{n}(MR_{pre,i} - MR_{exp,i})^2}{N}\right]^{1/2} \quad (5.3)$$

In which; MRexp, represents experimentally moisture ratio observed in the ith term, MRpre, represents moisture ratio projected in the ith term, N represents the number of the observations of experiments, and the n represents number of constants.

Table 5.1: Mathematical models are commonly used to explain the kinetics of drying.

No. of model	Name of model	Model	Reference
1	"Midilli" & "Kucuk" model	MR=a exp(-kt^n)+ bt	[35]
2	Verma model	MR=a exp(-kt)+(1-a) exp(-gt)	[34]
3	Modified Henderson and Pabis model	MR=a exp(-kt)+b exp(-gt)+c exp(-ht)	[33]
4	Diffusion approach model	MR=a exp(-kt)+(1-a) exp(-kbt)	[32]
5	Wang and Singh model	MR=1+at+at^2	[31]
6	Two- term exponential model	MR=a exp(-kt)+(1-a) exp(-kat)	[30]
7	Two term model	MR=a exp(-kt)+b exp(-k1t)	[29]
8	Logarithmic model	MR=a exp(-kt)+c	[28]
9	Henderson and Pabis model	MR=a exp(-kt)	[27]
10	Modified page model	MR=exp(-(kt)^n)	[26]
11	Page model	MR=exp(-kt^n)	[25]
12	Newton model	MR=exp(-kt)	[24]

5.3 The drying curves

Figure 5.1 Depicts saturated desiccant composite drying curves. The starting content of moisture (Mo) based on dry in desiccant composite is of 0.189kg of water per kg of dry desiccant and reduces progressively by the given drying period. Throughout investigation, drying didn't happen at the estimate of content, as illustrated in Figure 8 & 9.

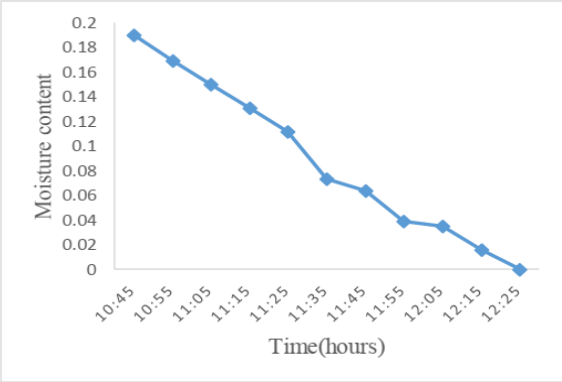

Figure 5.1: The graph depicts the change in availability as a function of drying time.

The surface of material is no more saturated by the water throughout the reducing rate period of the material, and also the rate of drying is regulated through diffusion of the moisture from inside of the solid surface [36].

5.4 Mathematical analysis of the solar drying curve

For statistical analysis of the drying models which is listed in Table 5.1, and the consequences are illustrated in Table 5.2, the MATLAB is used. R and RMSE are making use for evaluating the models. As demonstrated in Figure 5.2 and Table 5.2, the best descriptive model for desiccant composite is the Kucuk and Midilli model. The desiccant composite model of Kucuk and Midilli yields R = 0.9942 and RMSE = 0.03124.

Table 5.2 : The results of the statistical analyses on moisture ratio modeling based on drying time.

Model No.	Model name	Model constants	R	RSME
1	Newton	k =1.126	0.9308	0.0900
2	Page	k =1.195; n =1.632	0.9889	0.0380
3	Modified page	k =1.115; n = 1.632	0.9889	0.0380
4	Henderson and Pabis	a =1.093; k = 1.235	0.9441	0.0853
5	Logarithmic	a =2.545; c =-1.524; k = 0.3106	0.9919	0.0344
6	Two term	a = -37.36; b = 38.44; k_0 =0.573; k_1 =0.5876	0.9728	0.0674
7	Two-term exponential	a =2.032 ;k =1.827	0.9808	0.0499
8	Wang and Singh	a =-0.7353 b =0.07816	0.9916	0.0331
9	Diffusion approach	a =96.51; b = 0.9621; k = 0.1649	0.9911	0.0361
10	Modified Henderson and Pabis	a =-44.64;b = 0.01739; c =45.69; g =0.8484 ; h =1.532; k =1.542	0.9496	0.1087
11	Verma et al.	a =66.96;g =0.5364; k = 0.5434	0.9629	0.0737
12	Midilli and Kucuk	a=0.99; b=-0.0969; k =0.8506; n =1.409	0.9942	0.0312

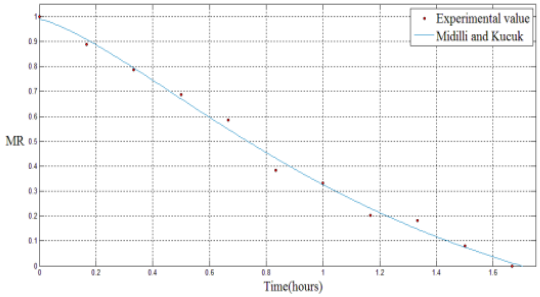

Figure 5.2: MATLAB was used to fit the curve of experimental moisture ratio value with drying time using the "Midilli and the Kucuk" model.

5.5 Conclusion

The data of moisture ratio is transformed to the usable moisture ratio (dimensionless term), and calculations on drying models of supplied for the curve fitting by many researchers from the drying time are performed. To describe the behavior of the new desiccant composite drying, 12 drying models are used. For statistical studies on drying models, MATLAB is utilized. With a R value 0.9942 and the RSME value of 0.03124, the "Kucuk and Midilli" model is selective model for better explanation in this situation.

6. Conclusions and the recommendations

6.1 Conclusion

The resurgence of the different desiccants has been found by using the direct heat through the solar concentrator of scheffler in aforementioned work. On the basis of consideration the cessations are sum up as illustrated:

The temperature of surface, which is contrived by intensity of sun and speed of wind, influences desiccant resurgence via physical heat utilized by the solar concentrator of scheffler. If resurgence is executed by utilizing direct heat through a solar concentrator of scheffler, the humidity ratio of air has no influence on desiccant resurgence. Moisture availability in silica gel, operated alumina, the molecular strain, the operated charcoal, and new composite are 0.2945, 0.0672, 0.2235, 0.057, and 0.18 kg for en example of same weight, but different desiccants (on the basis of wet) correspondingly, water per kg dry desiccant.

Because the silica gel having the highest adsorption potential of any desiccant studied, it is the best desiccant for utilize in the building of air dehumidification and also air conditioning. Because of its high moisture availability (somewhat lower compared to silica gel and also molecular strain) and resurgence for short time, new desiccant is a viable replacement for traditional desiccant. Operated alumina, silica gel, the molecular strain, operated charcoal, and new desiccants composite regenerates in 90, 160, 140, 120, and 110 minutes, respectively.

In the resurgence from a 1.53m^2 solar concentrator of scheffler, the greatest temperature of

surface is reached in the case of molecular sieve, 194.3^{0}C, and the highest rate of resurgence is achieved in the case of new desiccant composite, i.e. a rate of 0.07440kg/hr.

To describe the behavior of new composite desiccant drying, 12 drying models are used. With an RSME of 0.03124 and an R of 0.9942, the best descriptive model in this situation is the "Midilli and Kucuk" model.

6.2 Advice for the future work

The current study focuses on the designing of a solar concentrator of scheffler and the resurgence of different composite desiccant materials and saturated solid utilizing a scheffler sun concentrator. The composite desiccant drying curve has also been analytically modeled.

However, there are several additional concerns which may be examined. The following studies are suggested for the future:

1. Consolidation of solar concentrator of scheffler considering an air conditioning unit.

2. System's Implementation analysis by using the software as COMSOL, ANSYS etc.

3. Analytical analysis and the manufacturing of desiccant bed through desiccant composite for low temperature of resurgence.

REFERENCES

[1]. Rowland, C.A., and M.J. Wendel Jr., Equipment Notebook Dehumidification Technologies, 2005, HPAC Engineering.

[2]. J. Jeong, S. Yamaguchi, K. Saito, and S. Kawai, 2011. Analysis of the performance of desiccant dehumidification devices powered by low-grade heat International Journal of Refrigeration, 34(4).

[3]. M. Dupont, B. Celestine, P.H. Nguyen, J. Merigoux, and B. Brandon, 1994.I-dynamic experimental and computational investigations of silica gel and activated alumina for desiccant sun air cooling in tropical regions, Solar Energy, 52(6).

[4]. Singh, S., and P.P. Singh, 1998, Resurgence of silica gel in a multi-shelf regenerator renewable energy, vol. 13.

[5]. Techajunta, S., Chirarattananon, S., and R.H.B. Exell, 1999. Experiments on solid desiccant resurgence and air dehumidification in a sun simulator for air conditioning in a tropical humid region, Renewable Energy, vol. 17, no. 4.

[6]. S. Chindaruksa, J. Hirunlabh, and J. Khedari, 2001.Design of silica gel beds with active adsorption and passive resurgence for a drying system. Naresuan Warasan Mahawitthayalai.

[7]. S. Pramuang and R.H.B. Exell, 2007. Air from a solar heater with a compound parabolic concentrator is used to regenerate silica gel desiccant. Renewable Energy, Vol. 32, No. 1.

[8]. A. Kumar, A. Chaudhary, and A. Yadav, 2014.An experimental research of the resurgence of several solid desiccants utilizing a parabolic dish collector and adsorption rate.11th International Journal on Green Energy (9).

[9]. Yadav, A., and V.K. Bajpai, 2012. Experimental comparison of several solid desiccants for resurgence by evacuated solar air collector and air dehumidification.516-525 in Drying Technology, 30(5).

[10]. T.F.N. Thoruwa, C.M. Johnstone, A.D. Grant, and J.E. Smith, 2000. Desiccants based on $CaCl_2$ that are novel and inexpensive in cost for sun crop drying applications. Renewable Energy, Vol. 19, No. 4.

[11]. Thoruwa, T.F.N., Smith, J.E., Grant, A.D., and C.M. Johnstone, 1996.Sun drying advancements utilizing forced ventilation and solar regenerated desiccant materials. Renewable energy, vol. 9.

[12]. Zhang X.J., Sumathy K., Dai Y.J., and Wang R.Z., 2005. The fractal BET adsorption isotherm was used to conduct a parametric analysis on the silica gel–calcium chloride composite desiccant rotary wheel. International journal of energy research, volume 29, number 29. (1).

[13]. X.J. Zhang, K. Sumathy, Y.J. Dai, and R.Z. Wang, 2006. The hygroscopic dynamic impact of a composite material utilized in desiccant rotary wheel.

[14]. Tretiak, C.S., and N.B. Abdallah, 2009. A packed bed of clay-$CaCl_2$ desiccant particles' sorption and desorption properties Solar Energy, vol. 83, no. 10.

[15]. K.C. Chan, C.Y. Chao, G.N. Sze-To, and K.S. Hui, 2012.Predictions regarding the performance of a novel zeolite 13X/CaCl2 composite adsorbent for adsorption cooling systems. International Journal of Heat and Mass Transfer vol. 55, No. 1. (11).

[16]. Kumar, M., and A. Yadav, 2015. Experimental research of solar-powered water generation from atmospheric air using a composite desiccant material $CaCl_2$ or saw wood.

[17]. Kumar, A., and A. Yadav, Experimental examination of a solar-powered desiccant cooling system utilizing a composite desiccant "CaCl2/jute." in Environment, Development, and Sustainability.

[18]. Scheffler, W., Bruecke, S., and von Werdenbergstr, G., 2006, July, "Introduction to the innovative design of Scheffler reflectors," In 2006 Solar Cookers and Food Processing International Conference, Granada, Spain, July.

[19]. Munir, A., Hensel, O., and W. Scheffler, "Design concept and calculations of a Scheffler fixed focus concentrator for medium temperature applications", Solar Energy, vol. 84.

[20]. Dafle, V.R., and N.N. Shinde, 2012, "Design, Development, and Performance Evaluation of Concentrating Monoaxial Scheffler Technology for Water Heating and Low Temperature Industrial Steam Application", International Journal of Mechanical Engineering. The International Journal of Engineering Research and Applications (IJERA), vol. 2.

[21]. Holman, J. P., Experimental Methods for Engineers, McGraw-Hill, 1994.

[22]. A. Midilli and H. Kucuk, 2003. Mathematical simulation of pistachio thin layer drying utilizing solar energy. The Journal of Energy Conversion and Management, 44(7).

[23]. A.S. Mujumdar Industrial drying handbook The CRC Press.

[24]. L.M. Diamante and P.A. Munro, 1993. The thin layer sun drying of sweet potato slices was mathematically modeled. Solar energy.

[25]. G.M. White, T.C. Bridges, O.J. Loewer, and I.J. Ross, 1978. Seed coat loss during thin layer drying of soybeans as a result of drying conditions 34th ASAE Journal, New York, USA (3052).

[26]. Zhang, Q., and J.B. Litchfield, 1991. An investigation into the optimization of intermittent corn drying in a laboratory size thin layer drier. Drying Technology, vol. 9, no.

[27]. A. Yagcioglu, A. Degirmencioglu, and F. Cagatay, May 1999. The drying characteristics of laurel leaves under various circumstances. Proceedings of the Seventh International Congress on Agricultural Mechanization and Energy Vol. 26, No.

[28]. Henderson, S.M., 1974, Progress in the development of the thin layer drying equation. ASAE Transactions.

[29]. Sharaf-Eldeen, Y.I., Blaisdell, J.L., and Hamdy, M.Y., 1980. A model for drying ear corn. ASAE Transactions.

[30]. Wang, C.Y., and R.P. Singh, 1978, A single layer drying equation for rough rice (No. 78-3001). Paper for the ASAE.

[31]. A.S. Kassem, A.S. Kassem, A.S. Kassem, A.S. Kassem, A.S. Kassem Studies comparing thin layer drying models for wheat. In the Proceedings of the Thirteenth International Congress on Agricultural Engineering (Vol. 6, pp. 2-6).

[32]. V.T. Karathanos, 1999, Determination of water content in dried fruits using drying kinetics. 337-344 in Journal of Food Engineering, 39(4).

[33]. L.R. Verma, R.A. Bucklin, J.B. Endan, and F.T. Wratten, 1985. The impacts of drying air characteristics on rice drying models are investigated. ASAE Transactions.

[34]. A. Midilli, H. Kucuk, and Z. Yapar, 2002. A novel single-layer drying model.

[35]. L.M. Diamante and P.A. Munro, 1993, Mathematical modeling of thin layer sun drying of sweet potato slices. Solar energy, vol. 51, no. 4.

[36]. Ertekin, C. and Yaldiz, O., 2004. Drying of eggplant and selection of a suitable thin layer drying model. Journal of food engineering.

[37]. P. Vivekh, M. Kumja, D.T. Bui, and K.J. Chua. A overview of recent advances in solid desiccant coated heat exchangers. Appl Energy 2018;229:778–803. doi:10.1016/j.apenergy.2018.08.041.

[38]. D. Ürge-Vorsatz, L. F. Cabeza, S. Serrano, C. Barreneche, and K. Petrichenko. Building heating and cooling energy trends and drivers 2015, 41:85–98, Renew Sustain Energy Rev. https://doi.org/10.1016/j.rser.2014.08.039.

[39]. L. Wells, B. Rismanchi, and L. Aye. A study of net zero energy buildings with considerations for the Australian context. EnergyBuild2018;158:616–28, doi:10.1016/j.enbuild.2017.10.055.

[40]. Cooling in the Future. Energy - efficient air-conditioning opportunities in 2019 https://www.iea.org/futureofcooling/. [Accessed on the 19th of October, 2019].

[41]. Ma Y, Saha SC, Miller W, Guan L. Solar-assisted air cooling system comparison for Australian office buildings. Energies 2017; 10(10):1463. Doi: 10.3390/en10101463.

[42]. Jia CX, Dai YJ, Wu JY, and Wang RZ. A hybrid desiccant air-conditioning system is being studied. Application Therm Eng 2006;26(17–18):2393–400. https://doi.org/10.1016/j.\sappIthermaleng.2006.02.016.

[43]. D. La, Y. Dai, Y. Li, T. Ge, and R. Wang. A case study and theoretical analysis of a solar-powered two-stage rotary desiccant cooling system with vapour compression air-conditioning are presented.SolarEnergy,85(11),pp.2997–3009. https://doi.org/10.1016/j.solener.2011.08.039.

[44]. Jani DB, Mishra M, and Sahoo PK are the authors. The performance of a hybrid solid desiccant-vapor compression air-conditioning system is predicted using an artificial neural network. Energy2016,103(6):618–29. https://doi.org/10.1016/j.energy.2016.03.014.

[45]. Performance analysis of a two-stage desiccant cooling system, Tu R, Liu XH, Jiang Y. Applied Energy 113:1562–74, 2014. https://doi.org/10.1016/j.\sapenergy.2013.09.016.

[46]. Jiang GD, San JY. A silica gel packed-bed system was modeled and tested. International Journal of Heat Mass Transfer 1994; 37(8):1173–9. Doi: 10.1016/0017-9310(94) 90203-8.

[47]. MA Rady. The performance of dehumidifying desiccant beds made of silica-gel and thermal energy storage particles has been studied experimentally and numerically. Heat Mass Transfer, 45(5), 545 (2009). https://doi.org/10.1007/s00231-008-0459-4.

[48]. A. Sproul, M. Goldsworthy, and X. Zhou. An internally cooled desiccant wheel's performance was investigated. Appl Energy 2018; 224:382–97, doi: 10.1016/j.

[49]. Performance analysis of a four-partition desiccant wheel and a hybrid dehumidification air-conditioning system, Jeong J, Yamaguchi S, Saito K, and Kawai S. International Journal of Refrigeration,2010;33(3):496–509. https://doi.org/10.1016/j.ijrefrig.2009.12.001.

[50]. Chen CH, Ma SS, Wu PH, Chiang YC, and Chen SL are the authors of this paper. Air conditioning system adsorption and desorption of silica gel circulating fluidized beds Applied Energy 155:708–18, 2015. https://doi.org/10.1016/j.apenergy.2015.06.